Sodium and Chlorine Ions as Part of the DNA Solvation Shell

Michael Feig and B. Montgomery Pettitt
Department of Chemistry and Institute for Molecular Design, University of Houston, 4800 Calhoun, Houston, Texas 77204-5641 USA

ABSTRACT   The distribution of sodium and chlorine ions around DNA is presented from two molecular dynamics simulations of the DNA fragment $d(C_5T_5) \cdot (A_5G_5)$ in explicit solvent with 0.8 M additional NaCl salt. One simulation was carried out for 10 ns with the CHARMM force field that keeps the DNA structure close to A-DNA, the other for 12 ns with the AMBER force field that preferentially stabilizes B-DNA conformations (Feig and Pettitt, 1998, *Biophys. J.* 75:134–149). From radial distributions of sodium and chlorine ions a primary ion shell is defined. The ion counts and residence times of ions within this shell are compared between conformations and with experiment. Ordered sodium ion sites were found in minor and major grooves around both A and B-DNA conformations. Changes in the surrounding hydration structure are analyzed and implications for the stabilization of A-DNA and B-DNA conformations are discussed.

INTRODUCTION

Solvent effects play a significant role in the structure of DNA (Saenger, 1984). Hydration is essential in stabilizing the double helical form (Westhof, 1988) and this is particularly true for the biologically relevant B-DNA conformation (Harmouchi et al., 1990). Ions play an important role in DNA structure by shielding the phosphate charges in the DNA backbone and affecting water activity around DNA (Wang, 1955; Kubinec and Wemmer, 1992; Rau and Parsegian, 1992; Urabe et al., 1990; Forester and McDonald, 1991). Increased salt concentrations favor the formation of A-DNA and Z-DNA over B-DNA (Saenger, 1984; Nishimura et al., 1986) and salt effects constitute major electrostatic contributions in the binding of ligands to nucleic acids (Misra et al., 1994; Olmsted, 1996).

According to counterion condensation theory the number of counterions per phosphate group bound to DNA is nearly independent of the ionic strength of the surrounding medium (Record et al., 1978; Manning, 1978). Over a wide range of ion concentrations, 76% of all counterions are found within approximately 7 Å from the DNA surface. Counterion condensation theory is based on the assumption of low salt concentrations. If it is applied, nevertheless, to relatively high salt concentrations, an increase in counterion association can be predicted (Manning, 1978), but the significance of this trend remains unclear due to increasing theoretical inconsistencies. Experiments on ^{23}Na quadrupole relaxation (Bleam et al., 1980, 1983; Braunlin et al., 1986) reveal 50–80% of the counterions bound to DNA varying little with concentration. However, it is not clear how "bound" ions in NMR quadrupole relaxation experiments are related to "bound" ions in Manning's counterion condensation theory for different salt concentrations (Sharp and Honig, 1995). Deviations from counterion condensation

theory predictions that are based on a simple line charge model have been found with more detailed models in computer simulations and electrostatic potential calculations (Sharp and Honig, 1995).

For short DNA fragments, electrostatic end effects were found to play an important role. Considering finite cylindrical models, rather than an infinite rod as in the counterion condensation theory, with point charges spaced along its axis (Olmsted et al., 1989, 1995) or embedded charge densities (Allison, 1994), ion concentrations or electrostatic potentials at the cylindrical surface were increasingly reduced toward the cylinder cap. These end effects are most pronounced for solutions with ionic strengths of 1–10 mM ranging over the length of 20 basepairs from the end of the cylinder (Olmsted et al., 1989; Allison, 1994). For higher ionic concentrations end effects were significantly reduced, involving only about five basepairs at 0.1 M (Allison, 1994). The theoretical results were confirmed by experimental data on sodium ion accumulation near DNA sequences with 20 and 160 basepairs from nuclear magnetic resonance (NMR) relaxation measurements (Stein et al., 1995). Under salt-free conditions, the average counterion association as measured by the ^{23}Na relaxation rate is 80% more around the 160-basepair fragment than around the 20-basepair fragment. At sodium concentrations of 0.2 M the difference is reduced to 40%, suggesting a similar decrease in end effects toward higher ionic concentrations, as predicted by the theoretical studies. Comparable results were also reported very recently around single-stranded DNA (Zhang et al., 1999).

Residences times of ions around long DNA sequences have also been determined from NMR relaxation measurements. Depending on temperature, salt concentration, and DNA sequence, values of 1 to 6 ns have been reported for residence times of sodium ions bound to DNA, i.e., typically within 4 Å from the DNA surface (van Dijk et al., 1987). The lowest residence times were found at elevated temperatures and high salt concentrations.

Although x-ray crystallography has been very successful in revealing ordered water molecules around DNA (Savage

and Wlodawer, 1986; Schneider and Berman, 1995; Wahl and Sundaralingam, 1997) this has not been the case for ions around DNA. It is generally difficult to distinguish sodium cations from water in crystallography, because both have the same number of electrons and the size difference between them is well beyond the resolution that can be achieved in crystal x-ray diffraction experiments on DNA at present. However, sodium cations may be identified from the orientation of surrounding water molecules that form a coordination shell. Yet only very few sodium ion locations have been reported around duplex DNA structures. Relevant for comparison in this study are sodium ions in crystal structures of dinucleotide steps (Seeman et al., 1976; Rosenberg et al., 1976; Camerman et al., 1976; Coll et al., 1987) that are located predominantly in the minor groove. Very recently, highly ordered solvent locations in the central narrow minor groove of the Drew-Dickerson B-DNA dodecamer sequence d(CGCGAATTCGCG)$_2$ that had been previously regarded as water sites were reinterpreted as at least partially occupied by sodium ions (Shui et al., 1998). Although the reported experimental resolution of 1.4 Å is far better than the typical range for similar experiments, the presence of sodium ions still could not be observed directly but has been inferred from valence calculations (Nayal and Di Cera, 1996) and supported by typical coordination numbers for sodium with DNA backbone atoms and surrounding water molecules. Chlorine ions are found even less frequently in crystal diffraction patterns, and we have found only one structure in the Nucleic Acid Database (Berman et al., 1992) with a chlorine ion in the vicinity of a thymine methyl group in d(CGATCG^{6me}ATCG)$_2$ (Baikalov et al., 1993).

Attracted by the phosphate charge, the cations are predominantly correlated to the phosphate oxygens through the first hydration shell, but from Poisson-Boltzmann electrostatic potential calculations (Jayaram and Sharp, 1989; Rajasekaran and Jayaram, 1994; Pack et al., 1993; Young et al., 1997; Gil Montoro and Abascal, 1998) attractive potentials are also found in the groove regions. Monte Carlo (Jayaram et al., 1990; Mills et al., 1992; Young et al., 1997) and molecular dynamics simulations (Forester and McDonald, 1991; Jayaram and Beveridge, 1996; Laughton et al., 1995; Young et al., 1997) have been used to characterize and model the ion atmosphere in atomic detail.

The most remarkable result from computer simulation studies is the recent observation of sodium ions occupying electronegative pockets within the spine of hydration in the minor groove of the central base step in the AATT region of d(CGCGAATTCGCG)$_2$ (Young et al., 1997) and in the grooves of triple helices (Weerasinghe et al., 1995). The ion location in duplexes was found between the carbonyl groups of the thymine bases on opposite strands that closely match the new results from crystallographic experiments mentioned above.

For a statistically meaningful representation of ion distributions around DNA in computer simulations, long simulation times are essential because of the small number of

ions compared to water molecules and their very long residence times (on the order of nanoseconds) around DNA. In this paper we will present an analysis of the structure and dynamics of sodium and chlorine ions around the DNA duplex fragment d(C$_5$T$_5$) · d(A$_5$G$_5$) from two molecular dynamics simulations. The simulations have been carried out for 10 and 12 ns with the most recent CHARMM and AMBER force fields, respectively. An analysis of the DNA structure (Feig and Pettitt, 1998) and hydration patterns (Feig and Pettitt, 1999) has been presented elsewhere. In this paper we use the terms "CHARMM simulation" and "AMBER simulation" to denote simulations with our own simulation program while using the respective force field parameters. We found that the CHARMM force field constricts the DNA structure mostly to A-DNA conformations, whereas the AMBER force field preferentially promotes B-DNA features. With all other environmental conditions the same, the different average force field induced DNA conformations in the two simulations allow direct comparison of solvation structures around B- and A-DNA conformations. The length of the simulations presented is significantly longer than previous simulations that were concerned with ions around DNA. Furthermore, because of the excess salt we can present chlorine ion distributions around DNA that have not been shown before, because previous DNA simulations included counterions only. Due to the excess salt the ion concentration in this study is approximately 1 M. Although this concentration is relatively high compared to most experimental studies, it lies in the vicinity of the midpoint for the salt-induced transition from B- to A-DNA. A-DNA conformations have been found in solutions with 1 M salt and above (Nishimura et al., 1986; Wang et al., 1989), whereas in salt concentrations below 1 M. B-DNA is usually prevalent (Benevides et al., 1986; Nishimura et al., 1986; Rinkel et al., 1986; Wolk et al., 1989). Together with the bias from the CHARMM and AMBER force fields toward A- and B-DNA, respectively, these conditions are most interesting for the investigation of salt effects on the equilibrium between A- and B-DNA conformations that are not very well understood and will be discussed in detail.

In the next section we sketch the simulation protocols and analysis methods used. Next we present the results, starting from a general perspective and proceeding to a more detailed picture of individual solvation structures. We finish with a discussion of the results and our conclusions.

METHODS

The simulation protocol has been described in detail previously (Feig and Pettitt, 1998); therefore, only an outline is presented here. The DNA decamer d(C$_5$T$_5$) · d(A$_5$G$_5$) was simulated with the latest AMBER and CHARMM force fields (Cornell et al., 1995; MacKerell Jr. et al., 1995) in a solvent of 2285 explicit TIP3P (Jorgensen et al., 1983) water molecules, 18 Na counterions, and 32 additional Na/Cl ion pairs (Roux et al., 1995), resulting in total ion concentrations of 1.2 M Na$^+$ and 0.8 M Cl$^-$. The ions were initially placed by replacing randomly chosen water molecules throughout the simulation box. Standard molecular dynamics techniques

were used, including periodic boundary conditions, the velocity Verlet integrator (Allen and Tildesley, 1987), and SHAKE (Ryckaert et al., 1977), to enforce holonomic intramolecular bond constraints and allow an integrator time step of 2 fs. Electrostatic interactions were calculated by means of Ewald summation technique to avoid cutoff effects (de Leeuw et al., 1980; Smith and Pettitt, 1994). The simulation program has been developed in our laboratory (Smith et al., 1996). A total simulation time of 10 ns was produced with the CHARMM force field, and of 12 ns with the AMBER parameters. From the analysis of the solute we concluded that convergence effects are visible on a time scale of several nanoseconds (Feig and Pettitt, 1998). A dynamic equilibrium was established at 3 to 4 ns, so we will not include the first 3 ns in the following analysis of the ion atmosphere.

Average ion distributions around the DNA solute were obtained in the same manner as water distributions, which are described elsewhere (Feig and Pettitt, 1999). Each configuration was translated and rotated such that the DNA best fits to the average DNA structure were centered and oriented along the z axis. Sodium and chlorine ions, including their nearest periodic images, were then counted on a 158 × 158 × 198 grid for the whole 3.95 × 3.95 × 4.95 nm³ simulation box. This corresponds to a grid resolution of 0.025 nm.

Ion residence times within a shell around DNA and at specific highly ordered locations have been calculated from a coordination correlation function approach that is commonly used for solvent residence time analysis around solutes in molecular dynamics simulations (Bruge et al., 1996; Brunne et al., 1993; Rocchi et al., 1997). A correlation function $c_\alpha(t)$ for solvent molecules within a confined area α, either a shell with a given radius or an ordered location, is defined as follows:

$$c_\alpha(t) = \frac{1}{N_{solv}} \sum_{i=1}^{N_{solv}} \frac{1}{N_{\alpha,i}} \sum_{t'=0}^{t_{max}} p_{\alpha,i}(t', t'+t)$$

where $p_{\alpha,i}(t', t'+t)$ is 1 when a solvent molecule i remains within the confined area from time t' to $t'+t$ and 0 otherwise. $p_{\alpha,i}$ is summed over the production time t_{max} of a simulation and normalized by the number of times $N_{\alpha,i}$ at which a solvent molecule i is found within the confined area. A 0 value is assumed if $N_{\alpha,i} = 0$. A second summation is done over all solvent molecules N_{solv} for which residence times are calculated. When areas are defined by sharp limits, solvent molecules located close to the boundary often leave the area and return on subpicosecond time scales due to thermal fluctuations. Since these rebinding events do not actually represent reordering of the solvent we will ignore such events if they occur in less than 1 ps. The function $c_\alpha(t)$ represents the average distribution of residence times. Ideally it follows an exponential decay for a two-state equilibrium. However, rapid thermal fluctuations result in higher values at short times and insufficient sampling of long times produces a non-exponential tail. An effective residence time is determined as the inverse slope of the linear region in $\ln(c_\alpha(t))$ by least-squares linear fitting.

We have introduced a convenient basepair-centered coordinate system in the hydration analysis to describe hydration sites relative to basepairs (Feig and Pettitt, 1999). We will also use this coordination system to report ordered ion sites. An illustration is shown in Fig. 1. The x axis is defined by connecting the centers of mass of each base calculated from the non-hydrogen atoms, excluding the sugar and phosphate backbone. The sum of the C4–C2 (pyrimidine) and C6–C2 (purine) vectors is then used to define the x–y plane and the z axis perpendicular to that plane. The y axis results from the cross product of the z and x axes pointing from the major groove to the minor groove.

RESULTS

The presentation of results begins with a general picture of sodium and chlorine ions around DNA constructed from average ion density distributions and radial distribution functions. We will then continue with a more detailed discussion of ordered ion sites in the grooves as part of
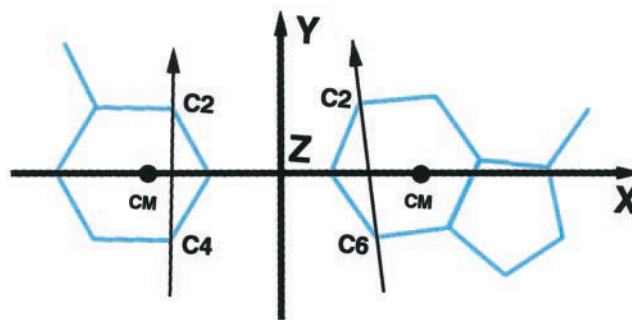

FIGURE 1   Basepair-centered coordinate system for description of solvent sites relative to basepairs.

DNA solvation and their implication in the stabilization of A- and B-DNA conformations.

Fig. 2 shows regions of elevated sodium and chlorine ion densities around the simulated average DNA structures in B and A conformations from the two simulations. Hydration patterns are shown for orientation and have been discussed elsewhere (Feig and Pettitt, 1999). Although the ordered water sites around DNA are populated for the largest part of the simulation time, this is not the case for the ions. Contours for the ion densities are shown at about 7.5 times fewer counts per time than those for the water oxygens, because none of the ion sites is populated more than a fraction of the simulation time. Also, no more than a few of the ion sites are occupied at any given time during the simulation, as will be seen later.

The most ordered sodium ions are generally located in the groove regions. Around the B-DNA structure from the AMBER force field, preferred sodium ion sites extend in the major groove along the guanine bases and along the spine of hydration in the narrow T · A minor groove. In the wider minor groove at C · G basepair, more confined sodium ion sites are visible between the guanine N2/N3 and the cytosine O2 atoms of the next basepair. This site is more populated at the second basepair (edge basepairs are omitted in the figure). Interestingly, at the third basepair a chlorine ion site has also been found at this location next to the sodium site, replacing the ordered water at the guanine N2 atom. Around the central C-T junction ordered ion sites are missing in the grooves, but the sodium ion density between backbone phosphates is noticeably elevated on the purine strand.

Different ion patterns are observed around the A-DNA structure from the simulation with CHARMM parameters. Most prominent is the sodium ion spine in the major groove along the purine bases. At the guanine bases a well ordered complex network is formed with the sodium surrounded by coordinated water molecules. At the third basepair the high sodium ion density extends to the water site at the guanine N7, indicating that a sodium ion is temporarily incorporated into the first solvation layer at this location. Chlorine ions are found in the C · G major groove at the cytosine N4 hydration site at the second and fourth basepairs. In the

FIGURE 2 Wall-eyed stereo view of sodium (red) ions and chlorine (green) ions around the simulated DNA fragment in B-DNA (*A*) and A-DNA (*B*) conformations from AMBER and CHARMM force field simulations. The sequence is oriented in both cases with C/G pairs on top and T/A pairs on the bottom. Water oxygens densities are shown for comparison in blue. Densities were averaged over 3–12 and 3–10 ns, respectively. Edge basepairs are omitted for clarity. Contours show ion densities at a level of 12 ions per nm^3. Water oxygen contours are plotted at 85 waters per nm^3 for the AMBER simulation and at 105 waters per nm^3 for the CHARMM simulation. For comparison, the bulk water number density corresponding to 1 g/cm^3 is 33 waters per nm^3.
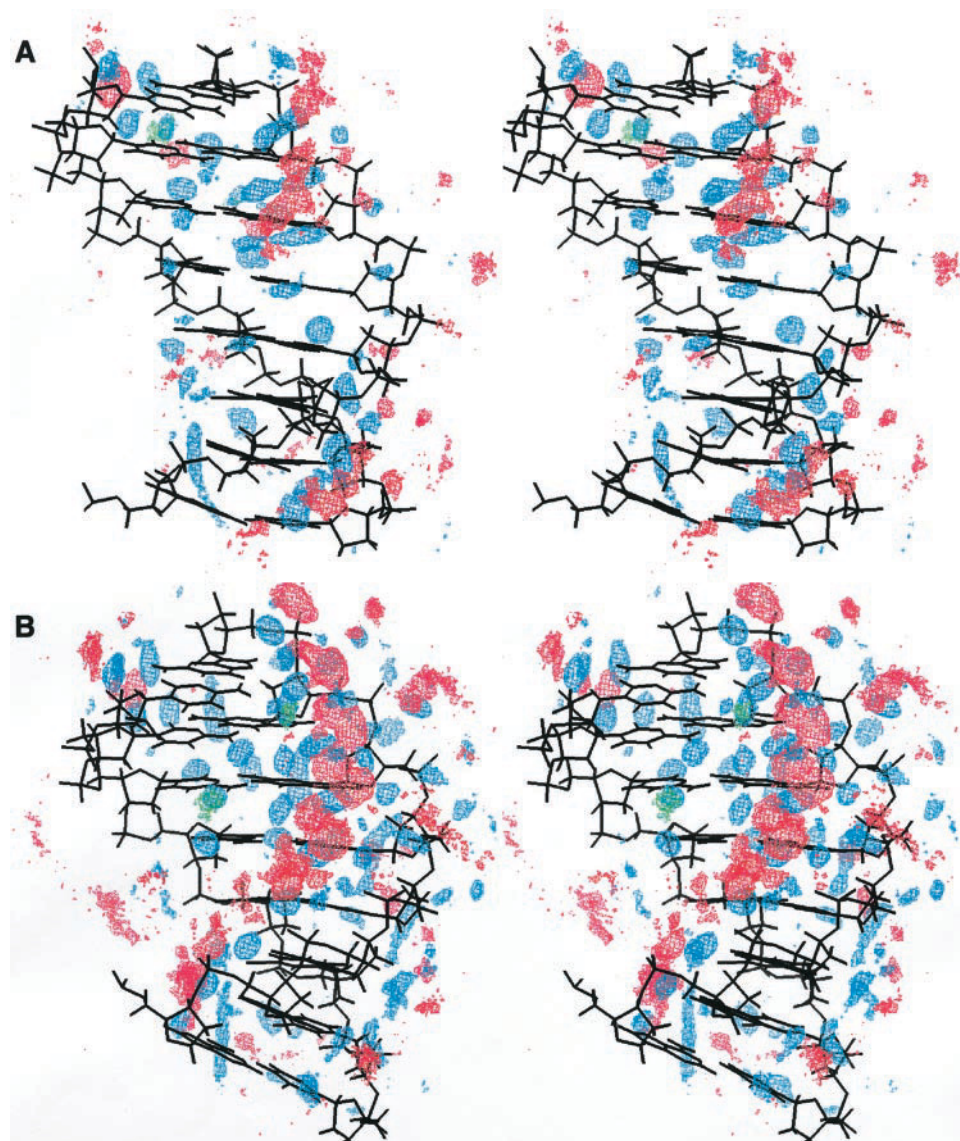
minor groove ordered ion sites are less well developed. Noticeable populations are present around the second C · G basepair and along the T · A basepairs in the center of the groove between basepairs at similar locations as around the B-DNA structure. Ion distributions around the backbone between successive phosphates are more visible at the purine strand in the CHARMM simulation, presumably because of a rigid backbone in A-DNA conformation throughout the simulation. In B form with the AMBER force field the backbone is more flexible, resulting in less defined surrounding solvent densities.

Radial distribution functions of ion distances to the closest heavy DNA atom are shown in Fig. 3, *A* and *B*. They are normalized by the available volume near a given distance from the closest DNA atom. The calculation of this normalization volume is nontrivial (Makarov et al., 1998a; Rudnicki and Pettitt, 1996). It has been determined the same way as in the normalization of radial water oxygen distributions (Feig and Pettitt, 1999), through a grid that contains

a list of the closest DNA atoms at each element and is updated every 10 configurations. Radial distributions of ions around DNA in the AMBER simulation have been shown before in a discussion of ion diffusion coefficients (Makarov et al., 1998b). The graphs shown here are averaged over a much longer part of the trajectory (9 ns vs. 200 ps) to provide a more detailed view and are also compared with the results from the CHARMM simulation. In addition, cumulative ion numbers depict the fraction of ions found within a given distance from the closest DNA atom. Sodium ions are most concentrated between the first and second hydration shells. The maximum of the radial distribution lies at 0.43 nm in the AMBER simulation and shifted slightly closer to the DNA at 0.415 nm in the CHARMM simulation. A second ion layer has its maximum at 0.645 nm from the closest DNA atom. In the simulation with the CHARMM force field, sodium ions also penetrate the first solvation layer (partially dehydrated), as can be seen from the small peak at 0.27 nm. Within 1 nm from the closest
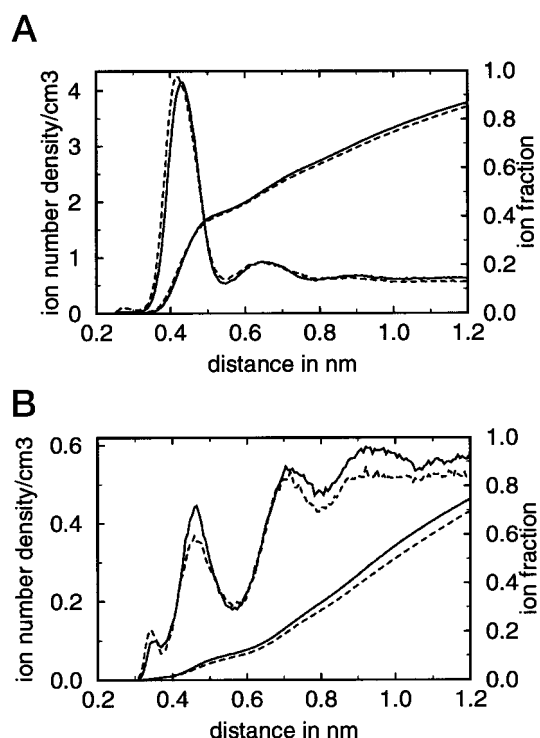
FIGURE 3 (*A*) Volume-normalized conditional radial distribution functions of sodium ion distances to the closest heavy DNA atom and cumulative sodium ion fractions within a given distance from the DNA from averages over the whole analyzed simulation time. *Solid* and *dashed lines* show results with AMBER and CHARMM force fields, respectively. Only ions closest to atoms in basepairs 2–9 were counted to exclude edge effects. (*B*) Volume-normalized conditional radial distribution functions and fractions of chlorine ions around DNA as in (*A*).

DNA atom 76.5% of all sodium ions are found. It should be noted that in our calculations of radial distributions and ion fractions we have not included the ions that are closest to the edge basepairs, to avoid end effects.

Radial distribution functions of chlorine ions around DNA have not been discussed before, primarily because most theoretical studies include only positive counterions. Even when chlorine ions are included, their small number close to the negatively charged DNA molecule, combined with short simulation times, does not provide statistically meaningful results. From the long simulations presented here with 0.8 M added NaCl salt an interesting profile emerges for chlorine ions around DNA. Due to the repulsion by the DNA charge their density remains below the bulk value for more than 1.5 nm distance from the closest heavy DNA atom with maxima at 0.345 nm, 0.465 nm, and 0.7 nm. As a consequence only 50 (CHARMM simulation) to 55% (AMBER simulation) of the chlorine ions are located within 1 nm from the closest DNA atom.

From the radial distribution functions the first ion shell can be defined by the minimum at 0.55 nm in both sodium and chlorine ion distributions. This is close to NMR criteria that consider ions bound within 0.4 nm from the DNA surface (Strzelecka and Rill, 1992). Note that our distance

criterion is relative to the closest heavy atom, whereas the DNA surface is commonly defined by all atoms, including hydrogen atoms. Therefore, distances relative to the DNA surface may be reduced by C-H and N-H bond lengths of 0.1 nm.

We have used this ion shell definition to count the number of ions around different functional groups and determine residence times around DNA. The average ion counts are given in Tables 1 and 2 for sodium and chlorine ions. From 1.6 to 1.8 sodium ions and 0.2 to 0.3 chlorine ions per basepair are found in the primary ion shell. The number of ions represent averages over 3–12 and 3–10 ns simulation times and should be interpreted in terms of populations.

More ions are counted around C · G basepairs than around T · A basepairs in both simulations. At the C-T junction the elevated number of sodium ions observed around the A form is remarkable. Most of the proximal sodium and chlorine ions are found around the phosphate groups, confirming expectations. The number (0.5 to 0.7) sodium ions per base at the phosphates agrees well with the 0.5 to 0.8 bound ions determined by NMR experiments (van Dijk et al., 1987; Strzelecka and Rill, 1992). From 0.05 to 0.1 chlorine ions are counted per base around the phosphate group. If this is interpreted in terms of populations it means that a chlorine ion is found at 5 to 10% of the time at a given phosphate group at this concentration. Significant sodium ion concentrations are observed in the major groove of both structures. Despite the much more prominent ordering of sodium sites around the A-DNA structure from the

TABLE 1   Sodium ion counts per basepair within 5.5 Å of the closest DNA atom

		AMBER	CHARMM
total	CC · GG	1.77 (1.16)	1.68 (1.11)
	CT · AG	1.68 (1.13)	1.76 (1.11)
	TT · AA	1.62 (1.06)	1.59 (1.07)
minor groove	CC · GG	0.06 (0.24)	0.06 (0.23)
	CT · AG	0.01 (0.11)	0.08 (0.27)
	TT · AA	0.03 (0.18)	0.08 (0.28)
major groove	CC · GG	0.31 (0.50)	0.25 (0.45)
	CT · AG	0.21 (0.43)	0.28 (0.48)
	TT · GG	0.21 (0.43)	0.20 (0.42)
phosphate	CC	0.66 (0.70)	0.53 (0.64)
	CT	0.60 (0.67)	0.53 (0.65)
	TT	0.65 (0.70)	0.51 (0.63)
	AA	0.57 (0.67)	0.53 (0.65)
	AG	0.73 (0.75)	0.63 (0.70)
	GG	0.63 (0.69)	0.67 (0.71)
sugar	CC	0.05 (0.22)	0.07 (0.25)
	CT	0.05 (0.21)	0.06 (0.24)
	TT	0.06 (0.24)	0.09 (0.30)
	AA	0.11 (0.32)	0.16 (0.38)
	AG	0.09 (0.30)	0.17 (0.39)
	GG	0.05 (0.23)	0.10 (0.30)

Ion counts are assigned to the structural subunits from the closest DNA atom. Values shown are averaged over basepairs 3 and 4 (CC · GG), 5 and 6 (CT · AG), and 7 and 8 (TT · AA) from 3–12 ns (AMBER) and 3–10 ns (CHARMM) simulation time. Root-mean-square fluctuations are given in parentheses.

TABLE 2 Chlorine ion counts per base pair within 5.5 Å of the closest DNA atom

		AMBER	CHARMM
total	CC · GG	0.28 (0.54)	0.20 (0.43)
	CT · AG	0.19 (0.42)	0.19 (0.43)
	TT · AA	0.19 (0.42)	0.16 (0.39)
minor groove	CC · GG	0.06 (0.23)	0
	CT · AG	0	0
	TT · AA	0	0
major groove	CC · GG	0.02 (0.13)	0.07 (0.25)
	CT · AG	0.01 (0.10)	0.01 (0.10)
	TT · GG	0.01 (0.10)	0
phosphate	CC	0.10 (0.30)	0.07 (0.25)
	CT	0.08 (0.27)	0.05 (0.23)
	TT	0.09 (0.29)	0.04 (0.20)
	AA	0.08 (0.29)	0.05 (0.22)
	AG	0.09 (0.29)	0.07 (0.26)
	GG	0.09 (0.28)	0.05 (0.22)
sugar	CC	0.01 (0.11)	0.01 (0.07)
	CT	0	0.01 (0.11)
	TT	0.01 (0.07)	0.02 (0.13)
	AA	0.01 (0.08)	0.04 (0.21)
	AG	0.01 (0.08)	0.04 (0.20)
	GG	0.01 (0.10)	0.02 (0.13)

Ion counts are assigned to the structural subunits from the closest DNA atom. Values shown are averaged over basepairs 3 and 4 (CC · GG), 5 and 6 (CT · AG), and 7 and 8 (TT · AA) from 3–12 ns (AMBER) and 3–10 ns (CHARMM) simulation time. Root-mean-square fluctuations are given in parentheses.

CHARMM simulation, the number of all ions closest to the major groove base atoms, at 0.2 to 0.3 per basepair, is actually slightly higher around the B-DNA form. This is partly explained by the location of the sodium sites close to the backbone in that often the closest atom is found within the sugar or phosphate groups rather than the major groove base atoms. This is confirmed by the elevated ion counts near the purine sugars and the guanine backbone compared to the pyrimidine strand. Chlorine ion counts in the groove regions reflect the ordered sites around C · G base pairs in the minor groove during the AMBER simulation and in the major groove during the CHARMM simulation. In general, the number of ions in the primary ion shell are quite similar around both structures, despite different patterns of ordered ions.

Using the coordination correlation function approach residence times were determined for sodium and chlorine ions within the primary shell. Fig. 4, *A* and *B,* shows the coordination correlation functions for sodium and chlorine in logarithmic scale. Linear regions with different slopes are found at short and intermediate time values. The shape of the correlation function for sodium ions in the AMBER simulation is less simple and possibly suggests a third linear region in between the other two. The observation of more than one linear region indicates processes at different time scales. By fitting linear functions to those linear regions residence times were estimated. They are listed in Table 3. The long residence times of sodium ions of approximately 1 ns agree well with the lower experimental values found
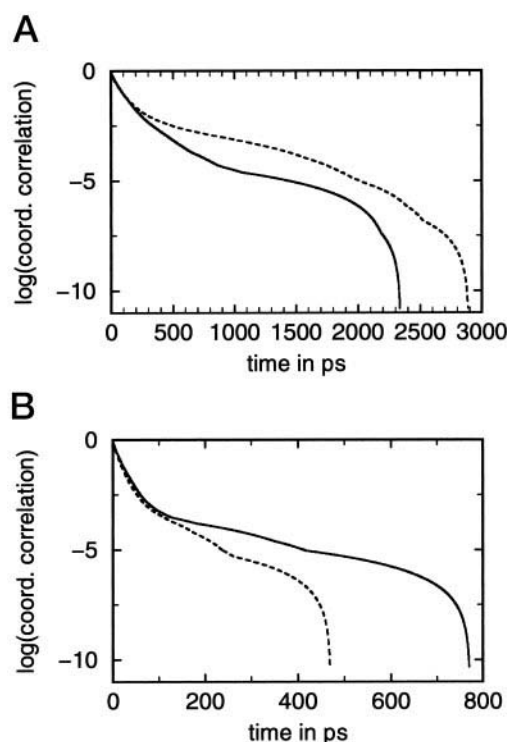

FIGURE 4 (*A*) DNA coordination correlation functions of sodium ions within 5.5 Å of the closest heavy DNA atom. Temporary exit and re-entry into this area around the DNA in less than 1 ps were ignored. *Solid* and *dashed lines* show different results with AMBER and CHARMM force fields. (*B*) DNA coordination correlation functions of chlorine ions as in (*A*).

from NMR relaxation measurements at 300 K and with added NaCl (van Dijk et al., 1987). Residence times of 100 to 200 ps were estimated for the chlorine ions. However, because of very low chlorine populations these results are statistically less meaningful than for the sodium ions.

We next discuss individual ordered ion sites from the DNA simulations. Increased sodium ion densities around the backbone along the bisector between phosphate groups have been extensively discussed before (Jayaram et al., 1990; Laughton et al., 1995; Young et al., 1997). We confirm these observations. However, the focus in this paper is on ordered ion sites in the minor and major grooves that are not as well understood. From the average ion densities shown in Fig. 2, ion site locations are determined at maxima of the three-dimensional density distributions.

TABLE 3 Ion residence times within 5.5 Å of the closest heavy DNA atom

Ion	Simulation	τ	Max
Na$^+$	AMBER	123, 280, 960	2342
	CHARMM	120, 930	2893
Cl$^-$	AMBER	24, 201	772
	CHARMM	22, 95	470

Times are given in picoseconds without considering subpicosecond re-entry events. Time values were calculated for linear regions in the coordination correlation function. Max, maximum observed residence time.

TABLE 4 Ordered sodium and chlorine ion sites in the grooves around B-DNA from the AMBER simulation

Ion	Location	Bases	Coordinates			Occupancy	τ	Maximum
Na$^+$	minor	gua:N2	2/3/4	0.28	0.61	−0.15	0.23/0.07/0.05	280/220/150	1094/352/246
		thy:O2	8/9	0.18	0.54	−0.13	0.07/0.10	97/93	318/155
		ade:N3	8/9	−0.04	0.64	0.06	0.06/0.10	75/57	266/190
	major	gua:O6	2/3/4	0.29	−0.58	0.12	0.19/0.16/0.25	28/15/36	113/67/150
		gua:N7	2/3/4	0.55	−0.62	0.12	0.13/0.12/0.11	14/28/25	67/100/115
Cl$^-$	minor	gua:N2	2/3	0.15	0.62	−0.03	0.08/0.04	223/148	653/310

The coordinates are given in nanometers relative to the basepair-centered coordinate system as explained in the text, averaged over the listed bases. Occupancies have been calculated from 3–12 ns simulation time. τ is the residence time in picoseconds estimated by fitting the linear region in the coordination correlation function. Ions are considered correlated within 0.25 nm from the density maximum of the closest site. Subpicosecond remigration events were ignored. Also given are maximum residence times (in picoseconds).

Occupancies and residence times for these ion sites are then calculated from ions found within 0.25 nm of the maximum of the closest of these sites. Tables 4 and 5 list the prominent ion sites that have been identified in minor and major grooves in both simulations. Due to the piecewise homopolymeric sequence of the simulated DNA fragment, most ion sites were found at the same relative location around different base pairs of the same base type, so their positions could be averaged. Occupancies and residence times are nevertheless given for each basepair to show the spread of values for an error estimate and a possible effect from the DNA edges and the C-T junction. None of the ion sites is fully occupied. Typical occupancies are 5 to 20% of the simulation time. Only for one sodium ion site at the guanine N7 atom in the major groove of the A-DNA structure from the CHARMM force field occupancy values reach 25 to 39%. Combined with a nearby second ion site, sodium is found close to the guanine N7 atom in the A-DNA conformation at 31 to 45% of the simulation time.

Around the B-DNA conformation simulated with the AMBER force field, ordered ion sites are found in the C · G and T · A minor grooves and in the C · G major groove. Toward the C-T junction the ion sites are less occupied or not occupied at all. Sodium and chlorine sites in the minor groove around C · G basepairs exhibit the longest observed residence times, 150 to 280 ps. However, except for the sodium at the second basepair, these sites are only rarely occupied. The sodium site is located somewhat between basepairs below the guanine N2 hydration water. The chlorine ion, on the other hand, replaces the guanine N2 water.

Fig. 5 shows a configuration where sodium and chlorine ions are found concurrently at the second and third basepairs, respectively. Ordered chlorine ions around the B-DNA structure are found only at the second and third C · G basepairs paired with a sodium ion at the neighboring base. Sodium as well as chlorine ions fit well with the minor groove hydration patterns. The largest change is the reorientation of the water molecules at the adenine N3 atom.

In the narrow T · A minor groove of the B-DNA conformer two different arrangements are found that incorporate a sodium ion into the solvation layer. In the first configuration the sodium ion is located between basepairs closer to the thymine O2 atom; in the second it lies in the base plane closer to the adenine N3 atom. Both configurations have nearly equal occupancies of 6 to 10%. Longer residence times are calculated for the sodium location between basepairs. This site also corresponds best with the location of sodium ions in the minor groove of d(CGCGAATTCGC)$_2$ that were found from x-ray diffraction analysis (Shui et al., 1998) and molecular dynamics studies (Young et al., 1997). Figs. 6 and 7 show the two configurations involving sodium in the T · A minor groove. In the first arrangement the sodium ion replaces the water bridge between adenine N3 and thymine O2 atoms of subsequent basepairs across the groove. Instead, water bridges are formed between O2 and N3 atoms to the O4′ atoms of the next sugar ring that are not commonly observed around the B-DNA structure when there are no ions present. These bridges pull the sugar groups on opposite strands together and cause the observed narrowing of the groove. In the

TABLE 5 Ordered sodium and chlorine ion sites in the grooves around A-DNA from the CHARMM simulation

Ion	Location	Bases	Coordinates			Occupancy	τ	Maximum
Na$^+$	minor	gua:N2	3	−0.06	0.66	0.12	0.12	83	289
		thy:O2	6/7	−0.06	0.68	0.05	0.12/0.10	28/41	110/193
		ade:N3	6/7/8	0.39	0.62	−0.14	0.09/0.15/0.15	38/29/35	125/111/157
	major	gua:N7	2/3/4/5	0.43	−0.62	0.09	0.39/0.25/0.29/0.25	160/92/96/124	586/343/370/340
		gua:N7	2/3/4/5	0.36	−0.44	0.18	0.06/0.06/0.16/0.13	19/19/42/65	53/56/147/158
		ade:N6	6/7/8	0.05	−0.65	0.05	0.12/0.14/0.13	31/21/32	118/106/131
		ade:N6	7/8	0.16	−0.64	0.15	0.10/0.15	18/28	80/161
		thy:C5M	7/8	−0.72	−0.55	−0.15	0.15/0.11	109/49	217/228
Cl$^-$	major	cyt:N4	2/4	−0.34	−0.54	−0.03	0.08/0.10	34/63	105/299

See Table 4 legend for explanation, except that these calculations are based on simulation time of 3–10 ns.

FIGURE 5   Wall-eyed stereo view of B-DNA C/G minor groove solvation from AMBER simulation at 3.3 to 3.6 ns simulation time around the third basepair. Water oxygen (blue), sodium (red), and chlorine (green) densities are contoured at number densities of 215 counts per nm^3. Water hydrogen densities are shown in grey at 260 counts per nm^3. Ions and water molecules were fitted to the densities for visual guidance.
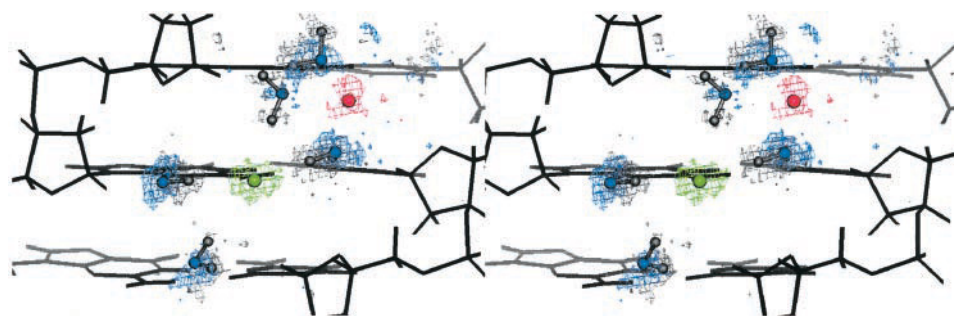
second arrangement the hydration structure is affected in a similar manner with a bridge also forming between the adenine N3 and the sugar O4′ as part of the ion solvation shell. It has been noted that the presence of an ion in the T · A minor groove decreases the groove width (Young et al., 1997). This effect is also observable in our simulations. A simple measure of the groove width is the distance between the opposing C1′ atoms of the glycosidic linkage for a given basepair. Table 6 shows the variation of C1′ distances at the presence of a sodium ion in the T · A minor groove. Three different time intervals are analyzed with a sodium ion between basepairs 7 and 8 and between 8 and 9 representative of the first structure and with sodium in the base plane of basepair 8 for the second type. In all cases a statistically significant reduction of the minor groove width is found. The incorporation of sodium in the first solvation shell between T · A basepairs leads to narrowing of the minor groove at the basepair below the ion toward the 3′ end of the pyrimidine strand, whereas the groove width of surrounding base pairs appears to be mostly unaffected. The DNA structure with a sodium ion in the base plane of the eighth base pair has a narrowed minor groove not just at the basepair where the sodium is located, but also at the neighboring base pairs, indicating a more extended effect on DNA structure than for the case where the ion is located between basepairs.

Two ion sites in the major groove of the B-DNA structure at the guanine O6 and N7 atoms are less well defined, with short ion residence times of 14 to 36 ps. However, they are occupied for 11 to 25% of the simulation time. Usually an ion is found at either one of these two sites, but we also observed the occupancy of both sites at the same time for extended periods of time. Figure 8 shows a picture of such

a sodium ion pair. The first layer hydration patterns are not altered significantly by the ions, because the O6–O6 and N7–N7 bridge waters as well as the cytosine N4 hydration site can provide the coordination shell in combination with second layer water molecules.

Ordered ion sites around the A-DNA conformation from the CHARMM force field simulation are particularly prominent in the major groove. They form a spine at the purine bases along the whole groove. However, different ion configurations are observed along the guanine and adenine bases. Furthermore, for both base types two close but distinct ion sites are identified. Combining the occupancies of both sites a sodium ion is found, on average, 31 to 45% of the simulation time at guanine bases and 22 to 29% of the time at adenine bases. Residence times around the guanine bases are up to 160 ps, but only 20 to 30 ps at adenine bases. The sodium ion site at the guanine base is located close to the N7 atom and close to the N6 atom at the adenine bases. Fig. 9 shows a picture of the C-T junction at a time where both sites at the adjacent guanine and adenine bases are concurrently occupied. Both ions keep the first hydration layer waters at the O6, N7, and cytosine N4 or thymine O4 sites mostly intact and cause additional ordering of second layer water molecules. Because of the high population of sodium ions at guanine bases, the ordered second layer waters are visible in average water density distributions as connected ring patterns along the guanine bases (Feig and Pettitt, 1999). Particularly interesting is the water bridge between successive phosphate groups that is stabilized by the sodium ion at guanine bases but not at adenine bases, as can be seen in Fig. 9. Water bridges between successive phosphates have been used to characterize A-DNA in comparison to B-DNA, where each phosphate group is individ-

FIGURE 6   B-DNA T/A minor groove solvation from AMBER simulation at 8.4 to 8.7 ns simulation time around the eighth basepair. Contour levels are as in Fig. 5.
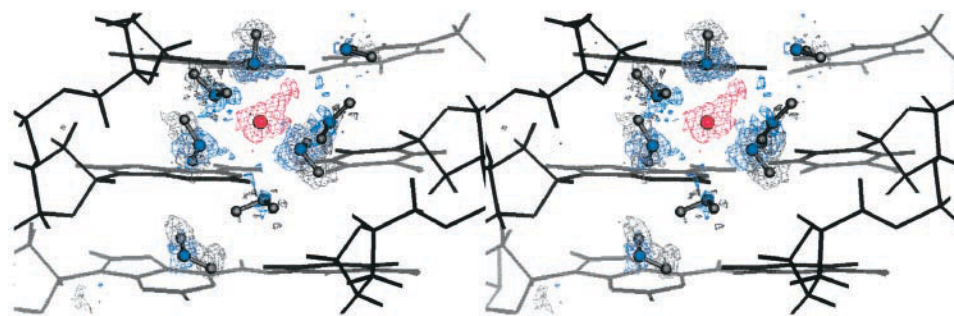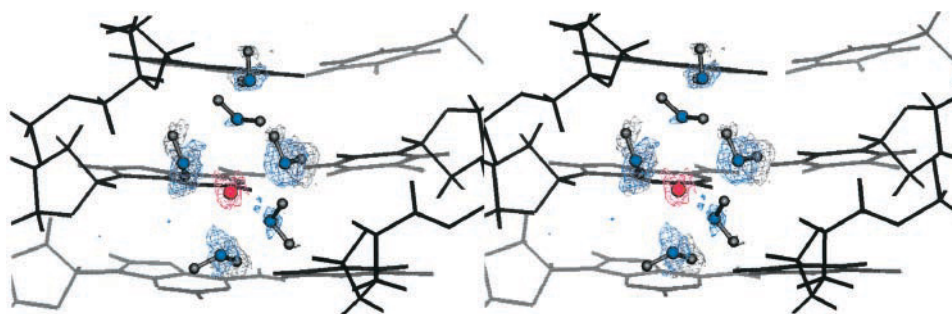
FIGURE 7 Alternative B-DNA T/A minor groove solvation arrangement from AMBER simulation at 8.7 to 9.6 ns simulation time around the eighth basepair. Contour levels are as in Fig. 5.

ually hydrated (Saenger, 1987). The arrangement of such bridges by ions in a major groove suggests an explanation how A-DNA is stabilized under high salt conditions.

Around the A-DNA form chlorine ions were found to form ordered sites only in the major groove close to the cytosine N4 atom. During the simulation these chlorine sites were occupied only at the second and fourth basepairs with residence times of 34 and 63 ps. Fig. 10 shows the solvation structure around the cytosine when a chlorine ion is present at the fourth basepair. It replaces the water at the N4 hydration site but does not induce ordered water sites as around sodium ions.

In the minor groove, sodium ion sites very similar to the ones around the B-DNA structure described above are also found around the A-DNA structure. However, their occupancies are higher, residence times are only half as long, and chlorine is not observed in the C · G minor groove of the A-DNA CHARMM simulation.

By comparing occupancy and residence time values for the same ion site at different basepairs it is possible to estimate upper bounds for statistical errors, because some of the variability might be caused by edge effects vicinity to the C-T junction. Coordinates are accurate within 0.03 nm. For occupancies standard deviations are generally between 0.04 and 0.06, in the C · G minor groove the standard deviation is 0.1. The estimated error in the residence times is between 10 and 60%.

DISCUSSION

From simulations over 10 ns presented here it is possible to provide a detailed discussion of sodium and chlorine ions around DNA at approximately 1 M salt concentration relevant to salt effects on the equilibrium between A- and B-DNA. Long residence times of around 1 ns in the primary ion shell and up to 280 ps in single ion sites, combined with a low frequency of ions entering the groove regions, require simulations of at least several nanoseconds after a sufficient equilibration period to arrive at a statistically meaningful picture. This could not be achieved in previous studies based on simulations from several hundred picoseconds to 1.5 ns (Forester and McDonald, 1991; Mohan et al., 1993; Young et al., 1997). Yet, even in simulations of 10 to 12 ns in length, as discussed here, some events, such as the presence of ordered ions in the C · G minor groove, are still not sampled sufficiently to provide accurate quantitative measures. However, due to the block-homopolymeric character of our simulated DNA fragment, averaging over two or three basepairs of the same type is possible to reduce the statistical error.

The discussion of ions around DNA in the past has been focused mainly on sodium counterion condensation around the negatively charged phosphate groups. Counterion condensation theory provides a mean field theoretical framework that describes the number of counterions bound to DNA per phosphate group under low salt conditions and for long DNA segments that can be compared to experimental numbers from ^{23}Na NMR relaxation studies (Sharp and Honig, 1995). Electrostatic end effects lead to reduced counterion association towards the ends of longer fragments and an overall reduction in very short fragments (Olmsted et al., 1989; Allison, 1994; Stein et al., 1995). Using more detailed models, simulations have located the sodium ions preferentially oriented along the bisector between phosphate

TABLE 6 Reduction of minor groove width at the presence of sodium in the minor groove of T · A basepairs 7–9 from the simulation with the AMBER force field

Basepairs	Time (ns)	Cl′–C1′ distance in Å		
		T · A 7	T · A 8	T · A 9
Total	4–12	10.63	10.59	10.52
Na⁺ @ T · A 7/8	8.55–8.58	−0.08 (0.13)	**−0.70** (0.13)	+0.01 (0.17)
Na⁺ @ T · A 8/9	7.75–7.9	−0.01 (0.08)	−0.06 (0.08)	**−0.13** (0.11)
Na⁺ @ T · A 8	8.8–9.2	**−0.14** (0.06)	**−0.21** (0.06)	**−0.16** (0.09)

As a measure of groove width, the distance between Cl′ atoms on opposing strands is used. Averages over short times with sodium present in the minor groove are represented as differences from the average over the total production time shown in the first line. Statistical errors of short time groove width averages are given in parentheses. Statistically significant deviations are indicated in bold type.

FIGURE 8 Sodium ion pair in B-DNA C/G major groove solvation shell from AMBER simulation at 11.2 to 11.3 ns simulation time around the third basepair. Contour levels are as in Fig. 5.
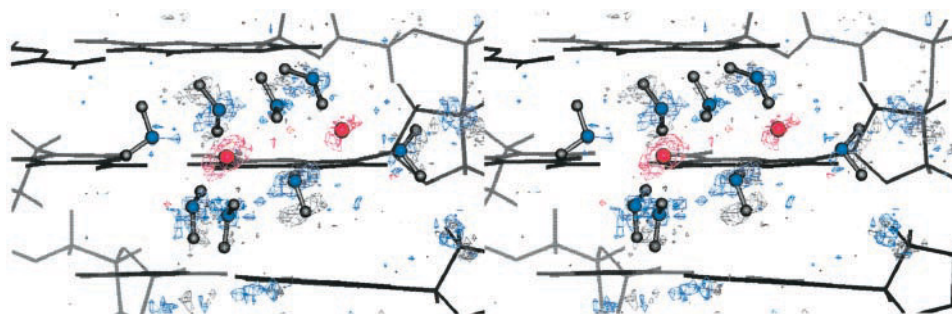
groups (Jayaram et al., 1990; Laughton et al., 1995). Recently interest has begun to shift toward ordered ions in the groove regions by the observation of sodium populations in the narrow minor groove along the AATT region of the dodecamer sequence d(CGCGAATTCCGCG)$_2$ in molecular dynamics simulations (Young et al., 1997) as well as experiments (Shui et al., 1998). The data presented here confirm these findings while proposing a more comprehensive picture of ordered ion sites in the DNA grooves. In addition, the added NaCl salt that was present in our simulation box provides the opportunity to discuss the distribution of chlorine ions around DNA, which has rarely been considered before (Rudnicki and Pettitt, 1996). Because the different force fields in our simulations stabilize B-DNA and A-DNA conformations with AMBER and CHARMM parameters, respectively, it was possible to make important comparisons between the ion structure around both conformations.

Radial distribution functions of ions relative to the DNA surface show primary and secondary ion coordination shells largely unaffected by the DNA conformation. Also, the number of ions within the primary shell is mostly similar around A- and B-DNA. Because a DNA fragment of only tenbase pairs is discussed here, electrostatic end effects would be expected to reduce the degree of ion association compared to the same sequence embedded in a much longer DNA fragment. However, although this effect is significant at low salt concentrations, theoretical (Allison, 1994) and experimental studies (Stein et al., 1995) suggest that this effect becomes much less important at concentrations of 0.1 and 0.2 M, and it is not clear to what extent sodium ion association is still affected by end effects at even higher concentrations of 1 M as simulated here.

Residence times within the primary ion shell were separated into 100-ps and 1000-ps time scales for sodium and 10-ps and 100-ps time scales for chlorine ions. They indicate different processes of ion-DNA association. The longer residence times of 930 to 960 ps for sodium ions agree well with experimental evidence in a high salt and environment at 300K (Groot et al., 1994; van Dijk et al., 1987). They are connected with ions that are incorporated into the solvation shell within the groove regions and then diffuse along the groove for extended periods of time before leaving the DNA and exchanging with the bulk solution. The shorter residence times of 120 ps characterize ions that are associated with the solvent-exposed phosphate oxygens. Similar residence times of 50 to 100 ps for sodium ions bound to phosphate oxygens have been reported before (Gulbrand et al., 1989). These calculated residence times may also be underestimated to the same extent as the distribution of ions, due to electrostatic end effects.

A detailed analysis of ordered ions in the groove regions has revealed distinct sites of localized ions that are sequence- and conformation-dependent. Most sites are occupied 10 to 30% of the simulation time, whereas residence times at single sites typically range from 20 to 200 ps. These ion sites are incorporated into the groove solvation structure by coordinating with first and second layer hydration water molecules. In order to arrange the required sixfold coordination shell around sodium, some of the highly ordered first layer waters are reoriented; a similar degree of order is imposed on other water molecules that are less ordered when ions are not present. Important for DNA structure are structural water bridges between DNA atoms that are formed to accommodate ions in the groove regions. This has been found in the T · A minor groove, where the central

FIGURE 9 A-DNA major groove solvation from CHARMM simulation at 6.0 to 6.1 ns simulation time around the central C-T junction. Contour levels are as in Fig. 5.
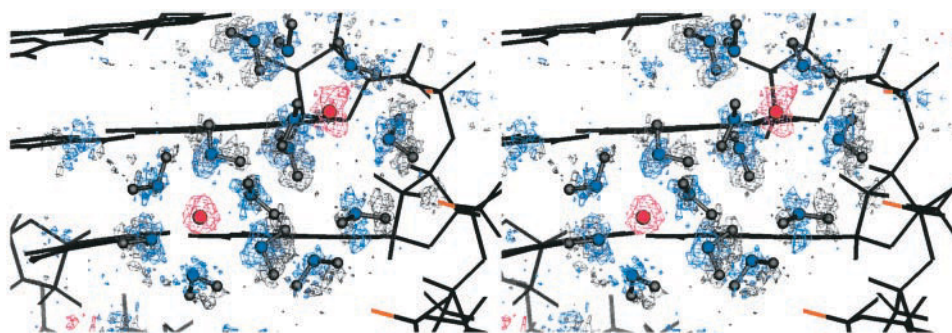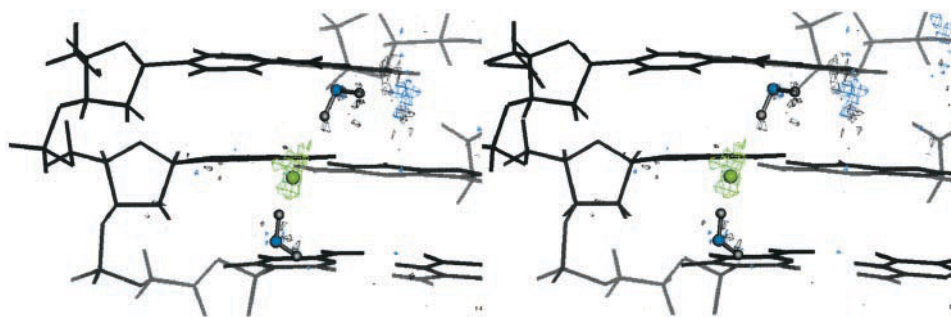
FIGURE 10 Chlorine ion site in A-DNA C/G major groove from CHARMM simulation at 8.7 to 9.0 ns simulation time around the fourth basepair. Contour levels are as in Fig. 5.

water that bridges adenine N3 and thymine O2 in successive base pairs across the groove is displaced by sodium and, instead, bridges are formed from the adenine N3 and thymine O2 atoms to the O4′ in the sugar of the next base in 5′ direction. This effect causes the minor groove to narrow and confirms a previous observation for sodium in the minor groove of AATT (Young et al., 1997).

In the major groove a well ordered spine of ion sites that are frequently populated extends along the DNA in the A but not the B conformation. Along the guanine bases the location of these ion sites at the N7 atom is close enough to the backbone to form a coordination shell that includes a well ordered water bridging successive phosphate oxygens. Along the adenine bases the location is moved toward the center of the major groove near the N6 atom, too far from the backbone to stabilize a water bridge between phosphates. Interphosphate water bridges are essential in the hydration of A-DNA conformations, whereas phosphate oxygens are hydrated individually in the B form. The observation of A-DNA at reduced water activities has been explained by a better "economy of hydration" with interphosphate water bridges that stabilize the A-DNA conformation (Saenger, 1987). Here, a modified explanation is offered for the transition to A-DNA in high salt environments by stabilizing interphosphate bridges through localized sodium ions in the major groove. Because this is not the case at adenine bases due to a shifted ion location, it would also explain why C · G base pairs undergo a B-to-A transition in 1 M NaCl solution (Nishimura et al., 1986), while A · T base pairs remain in B form even in higher salt concentrations (Wang et al., 1989). In addition, ions associated with the minor groove of A · T base pairs in B-DNA conformation cause the groove to narrow farther away from the transition point toward A-DNA. The stabilization of A-DNA through ion association at guanine bases in the major groove has been noted before in molecular dynamics simulations of d(ACCCGCGGGT)$_2$ in the presence of hexaamminecobalt(III) (Cheatham and Kollman, 1997). However, the stabilization of A-DNA was explained by the large, highly charged complex Co(NH$_3$)$_6^{3+}$ forming bridges between opposing strands across the major groove. These findings indicate an important structural role of explicit ions in the DNA groove regions in influencing the preference of DNA structures toward A and B conformations. They confirm and extend the results from an analysis of energy contributions in solvent-DNA interactions around A- and B-DNA structures that suggest the organization of counterions around DNA as a dominant factor in determining the preference for either the A or B form (Jayaram et al., 1998).

Chlorine ions have been found localized around C · G base pairs in the minor groove of the B-DNA conformation and in the major groove of the A-DNA form. They replace water molecules at the guanine N2 and cytosine N4 sites without altering the surrounding solvent structure significantly and were always paired with a sodium ion nearby along the minor groove or across the major groove, respectively. Although this is, to our knowledge, the first discussion of ordered chlorine ions around DNA, a significant contribution to DNA structure is not apparent from our simulations.

We note here that we have compared results from different force fields. We have used the tendency of CHARMM to yield A-like structures and AMBER to yield B-like structures as a mechanism to study different solvation patterns in DNA forms. We have not directly controlled for other differences the force fields might affect. However, to the extent that the individual characteristics of the force field accentuate the different DNA morphologies, they probably accentuate the solvation mechanisms causing the different preferences. It will be important to check these issues with the improved nucleic acid force fields that are currently being developed.

CONCLUSION

Molecular dynamics simulations in the 10-ns time regime reveal ordered sodium and chlorine ion sites in direct contact with the first hydration water molecules throughout minor and major grooves of A- and B-DNA conformations. The sodium ions in the DNA grooves induce ordering and reordering of surrounding water molecules to reach a six-fold coordination shell that has consequences for the stabilization of different DNA conformations. B-DNA is stabilized by ions associating with the minor groove of T · A basepairs that cause the reorientation of hydration water molecules to form bridges from adenine N3 and thymine O2 atoms to the sugar O4′ atom. The sugar groups are effectively pulled together across the groove and the consequence is a narrowed groove. For A-DNA the ion spine

along the purine bases in the major groove is most important. At the guanine bases ions are located close to the N7 atom, supporting well-ordered interphosphate water bridges that are essential in stabilizing A-DNA structures. Along the adenine bases the sodium ions are shifted more toward the center of the groove, too far from the backbone to stabilize interphosphate water bridges. This offers an attractive explanation of the experimentally observed preference of $T \cdot A$ base pairs for B-DNA even in very high salt conditions while $C \cdot G$ base pairs easily undergo a transition to the A form with increased salt concentrations.

REFERENCES

Allen, M. P., and D. J. Tildesley. 1987. Computer Simulation of Liquids. Oxford University Press, New York, 1st edition.

Allison, S. A. 1994. End effects in electrostatic potentials of cylinders: models for DNA fragments. *J. Phys. Chem.* 98:12091–12096.

Baikalov, I., K. Grzeskowiak, K. Yanagi, J. Quintana, and R. E. Dickerson. 1993. The crystal structure of the trigonal decamer C-G-A-T-C-G-^{6me}A-T-C-G: A B-DNA helix with 10.6 base pairs per turn. *J. Mol. Biol.* 231:768–784.

Benevides, J. M., A. H.-J. Wang, A. Rich, Y. Kyogoku, G. A. van der Marel, J. H. van Boom, and G. J. Thomas. 1986. The Raman spectra of single crystals of r(GCG)d(CGC) and d(CCCCGGGG) as model for A-DNA, their structure transitions in aqueous solution and comparison with double helical poly(dG) · poly(dC). *Biochemistry.* 25:41–50.

Berman, H. M., W. K. Olson, D. L. Beveridge, J. Westbrook, A. Gelbin, T. Demeny, S.-H. Hsieh, A. R. Srinivasan, and B. Schneider. 1992. The nucleic acid database: a comprehensive relational database of three-dimensional structures of nucleic acids. *Biophys. J.* 63:751.

Bleam, M. L., C. F. Anderson, and M. T. Record. 1980. Relative binding affinities of monovalent cations for double-stranded DNA. *Proc. Natl. Acad. Sci. USA.* 77:3085–3089.

Bleam, M. L., C. F. Anderson, and M. T. Record. 1983. ^{23}Na nuclear magnetic resonance studies of cation-deoxyribonucleic acid interactions. *Biochemistry.* 22:5418–5425.

Braunlin, W. H., C. F. Anderson, and M. T. Record. 1986. ^{23}Na-NMR investigations of counterion exchange reactions of helical DNA. *Biopolymers.* 25:205–214.

Bruge, F., E. Parisi, and S. L. Fornili. 1996. Effects of simple model solutes on water dynamics: residence time analysis. *Chem. Phys. Lett.* 250:443–449.

Brunne, R. M., E. Liepinsh, G. Otting, K. Wüthrich, and W. F. van Gunsteren. 1993. Hydration of proteins: a comparison of experimental residence times of water molecules solvating the bovine pancreatic trypsin inhibitor with theoretical model calculations. *J. Mol. Biol.* 231:1040–1048.

Camerman, N., J. K. Fawcett, and A. Camerman. 1976. Molecular structure of deoxyribose-dinucleotide, sodium thymidylyl-(5′-3′)-thymidylate-(5′) hydrate (pTpT), and a possible structural model for polythymidylate. *J. Mol. Biol.* 107:601–621.

Cheatham, T. E., and P. A. Kollman. 1997. Insight into the stabilization of A-DNA by specific ion association: Spontaneous B-DNA to A-DNA transitions observed in molecular dynamics simulations of d(AC-CCGCGGGT)$_2$ in the presence of hexamminecobalt(III). *Structure.* 15:1297–1311.

Coll, M., X. Solans, M. Font-Altaba, and J. A. Subirana. 1987. Crystal and molecular structure of the sodium salt of the dinucleotide duplex d(CpG). *J. Biomol. Struct. Dyn.* 4:797–811.

Cornell, W. D., P. Cieplak, C. I. Bayly, I. R. Gould, K. M. Merz, D. M. Ferguson, D. C. Spellmeyer, T. Fox, J. W. Caldwell, and P. A. Kollman. 1995. A second generation force field for the simulation of proteins, nucleic acids, and organic molecules. *J. Am. Chem. Soc.* 117:5179–5197.

de Leeuw, S. W., J. W. Perram, and E. R. Smith. 1980. Simulation of electrostatic systems in periodic boundary conditions. I. Lattice sums and dielectric constants. *Proc. R. Soc. Lond. A.* 373:27–56.

Feig, M., and B. M. Pettitt. 1998. Structural equilibrium of DNA represented with different force fields. *Biophys. J.* 75:134–149.

Feig, M., and B. M. Pettitt. 1999. Modeling high-resolution hydration patterns in correlation with DNA sequence and conformation. *J. Mol. Biol.* 286:1075–1095.

Forester, T. R., and I. R. McDonald. 1991. Molecular dynamics studies of the behaviour of water molecules and small ions in concentrated solutions of polymeric B-DNA. *Mol. Phys.* 72:643–660.

Gil Montoro, J. C., and J. L. F. Abascal. 1998. Ionic distribution around simple B-DNA models. II. deviations from cylindrical symmetry. *J. Chem. Phys.* 109:6200–6210.

Groot, L. C. A., J. R. C. van der Maarel, and J. C. Leyte. 1994. ^{23}Na relaxation in isotropic and anisotropic liquid-crystalline DNA solutions. *J. Phys. Chem.* 98:2699–2705.

Gulbrand, L. E., T. R. Forester, and R. M. Lynden-Bell. 1989. Distribution and dynamics of mobile ions in systems of ordered B-DNA. *Mol. Phys.* 67:473–493.

Harmouchi, M., G. Albiser, and S. Premilat. 1990. Changes of hydration during conformational transitions of DNA. *Eur. Biophys. J.* 19:87–92.

Jayaram, B., and D. L. Beveridge. 1996. Modeling DNA in aqueous solutions: Theoretical and computer simulation studies on the ion atmosphere of DNA. *Annu. Rev. Biophys. Biomol. Struct.* 25:367–394.

Jayaram, B., and K. A. Sharp. 1989. The electrostatic potential of B-DNA. *Biopolymers.* 28:975–993.

Jayaram, B., D. Sprous, M. A. Young, and D. L. Beveridge. 1998. Free energy analysis of the conformational preferences of A and B forms of DNA in solution. *J. Am. Chem. Soc.* 120:10629–10633.

Jayaram, B., S. Swaminathan, D. L. Beveridge, K. Sharp, and B. Honig. 1990. Monte carlo simulation studies on the structure of the counterion atmosphere of B-DNA. Variations on the primitive dielectric model. *Macromolecules.* 23:3156–3165.

Jorgensen, W., J. Chandrasekhar, J. Madura, R. Impey, and M. Klein. 1983. Comparison of simple potential functions for simulating liquid water. *J. Chem. Phys.* 79:926–935.

Kubinec, M. G., and D. E. Wemmer. 1992. NMR evidence for DNA bound water in solution. *J. Am. Chem. Soc.* 114:8739–8740.

Laughton, C. A., F. J. Luque, and M. Orozco. 1995. Counterion distribution around DNA studied by molecular dynamics and quantum mechanical simulations. *J. Phys. Chem.* 99:11591–11599.

MacKerell Jr., A. D., J. Wiorkiewicz-Juczera, and M. Karplus. 1995. An all-atom empirical energy function for the simulation of nucleic acids. *J. Am. Chem. Soc.* 117:11946–11975.

Makarov, V. A., B. K. Andrews, and B. M. Pettitt. 1998a. Reconstructing the protein-water interface. *Biopolymers.* 45:469–478.

Makarov, V. A., M. Feig, and B. M. Pettitt. 1998b. Diffusion of solvent around biomolecular solutes. A molecular dynamics simulations study. *Biophys. J.* 75:150–158.

Manning, G. S. 1978. The molecular theory of polyelectrolyte solutions with applications to the electrostatic properties of polynucleotides. *Q. Rev. Biophys.* 11:179–246.

Mills, P. A., A. Rashid, and T. L. James. 1992. Monte carlo calculations of ion distributions surrounding the oligonucleotide d(ATATATATAT)$_2$ in the B, A, and wrinkled D conformations. *Biopolymers.* 32:1491–1501.

Misra, V. K., K. A. Sharp, R. A. Friedman, and B. J. Honig. 1994. Salt effects on ligand-DNA binding. *J. Mol. Biol.* 238:245–263.

Mohan, V., P. E. Smith, and B. M. Pettitt. 1993. Molecular dynamics simulation of ions and water around triplex DNA. *J. Phys. Chem.* 97:12984–12990.

Nayal, M., and E. Di Cera. 1996. Valence screening of water in protein crystals reveals potential Na$^+$ binding sites. *J. Mol. Biol.* 256:228–234.

Nishimura, Y., C. Torigoe, and M. Tsuboi. 1986. Salt induced B-A transition of poly(dG) · poly(dC) and the stabilization of A form by its methylation. *Nucleic Acids Res.* 14:2737–2748.

Olmsted, M. C. 1996. The effect of nucleic acid geometry on counterion association. *J. Biomol. Struct. Dyn.* 13:885–902.

Olmsted, M. C., C. F. Anderson, and M. T. Record, Jr. 1989. Monte Carlo description of oligoelectrolyte properties of DNA oligomers: range of the end effect and the approach of molecular and thermodynamic properties to the polyelectrolyte limits. *Proc. Natl. Acad. Sci. USA.* 86:7766–7770.

Olmsted, M. C., J. P. Bond, C. F. Anderson, and M. T. Record. 1995. Grand canonical monte carlo molecular and thermodynamic predictions of ion effects on binding of an oligocation (L^8+) to the center of DNA oligomers. *Biophys. J.* 68:634–647.

Pack, G., G. Garrett, L. Wong, and G. Lamm. 1993. The effect of a variable dielectric coefficient and finite ion size on Poisson-Boltzmann calculations of DNA-electrolyte systems. *Biophys. J.* 65:1363–1370.

Rajasekaran, E., and B. Jayaram. 1994. Counterion condensation in DNA systems: the cylindrical poisson-boltzmann model revisited. *Biopolymers.* 34:443–445.

Rau, D. C., and A. Parsegian. 1992. Direct measurement of the intermolecular forces between counterion-condensed DNA double helices: evidence for long range attractive hydration forces. *Biophys. J.* 61:246–259.

Record, M. T., C. F. Anderson, and T. M. Lohman. 1978. Thermodynamic analysis of ion effects on the binding and conformational equilibria of proteins and nucleic acids: the roles of ion association or release, screening, and ion effects on water activity. *Q. Rev. Biophys.* 11:103–178.

Rinkel, L. J., M. R. Sanderson, G. A. van der Marel, and C. Altona. 1986. Conformational analysis of the octamer d(GGCCGGCC) in aqueous solution. *Eur. J. Biochem.* 159:85–93.

Rocchi, C., A. R. Bizzarri, and S. Cannistraro. 1997. Water residence times around copper plastocyanin: a molecular dynamics simulation approach. *Chem. Phys.* 214:261–276.

Rosenberg, J. M., N. C. Seeman, R. O. Day, and A. Rich. 1976. RNA double-helical fragments at atomic resolution: II. The crystal structure of sodium guanylyl-3′,5′-cytidine nonahydrate. *J. Mol. Biol.* 104:145–167.

Roux, B., B. Prodhom, and M. Karplus. 1995. Ion transport in the gramicidin channel: Molecular dynamics study of single and double occupancy. *Biophys. J.* 68:876.

Rudnicki, W. R., and B. M. Pettitt. 1996. Modeling the DNA-solvent interface. *Biopolymers.* 41:107–119.

Ryckaert, J. P., G. Ciccotti, and H. J. C. Berendsen. 1977. Numerical integration of the Cartesian equations of motion of a system with constraints: Molecular dynamics of n-alkanes. *J. Comput. Phys.* 23:327–341.

Saenger, W. 1984. Principles of Nucleic Acid Structure. Springer Verlag, New York.

Saenger, W. 1987. Structure and dynamics of water surrounding biomolecules. *Annu. Rev. Biophys. Biophys. Chem.* 16:93–114.

Savage, H., and A. Wlodawer. 1986. Determination of water structure around biomolecules using X-ray and neutron diffraction methods. *Methods Enzymol.* 127:162–183.

Schneider, B., and H. M. Berman. 1995. Hydration of the DNA bases is local. *Biophys. J.* 69:2661–2669.

Seeman, N. C., J. M. Rosenberg, and A. Rich. 1976. Sequence-specific recognition of double helical nucleic acids by proteins. *Proc. Natl. Acad. Sci. USA.* 73:804–808.

Sharp, K. A., and B. Honig. 1995. Salt effects on nucleic acids. *Curr. Opin. Struct. Biol.* 5:323–328.

Shui, X., L. McFail-Isom, G. G. Hu, and L. D. Williams. 1998. The B-DNA dodecamer at high resolution reveals a spine of water on sodium. *Biochemistry.* 37:8341–8355.

Smith, P. E., M. E. Holder, L. X. Dang, M. Feig, and B. M. Pettitt. 1996. Extended System Program, University of Houston, Houston, TX.

Smith, P. E., and B. M. Pettitt. 1994. Modeling solvent in biomolecular systems. *J. Phys. Chem.* 98:9700–9711.

Stein, V. M., J. P. Bond, M. W. Capp, C. F. Anderson, and M. T. Record. 1995. Importance of coulombic end effects on cation accumulation near oligoelectrolyte B-DNA: a demonstration using ^{23}Na NMR. *Biophys. J.* 68:1063–1072.

Strzelecka, T. E., and R. L. Rill. 1992. ^{23}Na NMR of concentrated DNA solutions: salt concentration and temperature effects. *J. Phys. Chem.* 96:7796–7807.

Urabe, H., M. Kato, and Y. Tominaga. 1990. Counterion dependence of water of hydration in DNA gel. *J. Chem. Phys.* 92:768–774.

van Dijk, L., M. L. H. Gruwel, W. Jesse, J. de Bleijser, and J. C. Leyte. 1987. Sodium ion and solvent nuclear relaxation results in aqueous solutions of DNA. *Biopolymers.* 26:261–284.

Wahl, M. C., and M. Sundaralingam. 1997. Crystal structures of A-DNA duplexes. *Biopolymers (Nucleic Acid Sci.).* 44:45–63.

Wang, J. H. 1955. The hydration of deoxyribonucleic acid. *J. Am. Chem. Soc.* 77:258–260.

Wang, Y., G. A. Thomas, and W. L. Peticolas. 1989. A duplex of the oligonucleotides d(GGGGGTTTTT) and d(AAAAACCCCC) forms an A to B conformational junction in concentrated salt solutions. *J. Biomol. Struct. Dyn.* 6:1177–1187.

Weerasinghe, S., P. E. Smith, V. Mohan, Y.-K. Cheng, and B. M. Pettitt. 1995. Nanosecond dynamics and structure of a model DNA triple helix in saltwater solution. *J. Am. Chem. Soc.* 117:2147–2158.

Westhof, E. 1988. Water: an integral part of nucleic acid structure. *Annu. Rev. Biophys. Biophys. Chem.* 17:125–144.

Wolk, S., W. N. Thurmes, W. S. Ross, C. C. Hardin, and I. Tinoco. 1989. Conformational analysis of d(C$_3$G$_3$), a B-family duplex in solution. *Biochemistry.* 28:2452–2459.

Young, M. A., B. Jayaram, and D. L. Beveridge. 1997. Intrusion of counterions into the spine of hydration in the minor groove of B-DNA: fractional occupancy of electronegative pockets. *J. Am. Chem. Soc.* 119:59–69.

Zhang, W., H. Ni, M. W. Capp, C. F. Anderson, T. M. Lohman, and M. T. Record, Jr. 1999. The importance of coulombic end effects: experimental characterization of the effects of oligonucleotide flanking charges on the strength and salt dependence of oligocation (L^8+) binding to single-stranded DNA oligomers. *Biophys. J.* 76:1008–1017.